



Amirkabir University of Technology
(Tehran Polytechnic)
Vol. 47, No. 1, Spring 2015, pp. 1- 10



Amirkabir International Journal of Science & Research
(Electrical & Electronics Engineering)
(AIJ-EEE)

A Probabilistic Three-Phase Time Domain Electric Arc Furnace Model based on analytical method

M. Torabian Esfahani¹ and B. Vahidi^{2*}

1- PhD. Student, Department of Electrical Engineering, Amirkabir University of Technology, Tehran, Iran
2- Professor, Department of Electrical Engineering, Amirkabir University of Technology, Tehran, Iran

ABSTRACT

An electric arc furnace (EAF) is known as nonlinear and time variant load that causes power quality (PQ) problems such as, current, voltage and current harmonics, voltage flicker, frequency changes in power system. One of the most important problems to study the EAF behavior is the choice of a suitable model for this load. Hence, in this paper, a probabilistic three-phase model is proposed based on recovered hidden Markov model (RHMM) in time domain. To recover the HMM, the coupling factor is proposed. This factor estimates the past observations and considers the effects of all observations in different states. Regarding to the intense fluctuations of various parameters of EAF, this factor can improve the EAF model in different operating stages. This subject causes that the proposed model is closed to the actual model. To train the RHMM, actual measured samples are used. Likewise, different parameters of EAF' power system as, flexible cables, electrode, busbar are exactly considering to achieve an accurate model. Comparing the results of experimental and proposed model indicates the accuracy of the proposed model.

KEYWORDS

Recovered Hidden Markov Model, Electric Arc Furnace, Voltage Flicker, Power Quality parameters.

*

Corresponding Author, Email: vahidi@aut.ac.ir

Vol. 47, No. 1, Spring 2015

1- INTRODUCTION

Electric arc furnaces (EAFs) are widely used in iron and steel industry. The operation performed by an EAF is smelting the scrap metal by generating arcs that can demand up to 120 MW. EAF operations and the induced voltage flickers are affected by melting materials, melting stage, electrode position, power supply voltage, and system impedance. On the other hand, the distortions and disturbance such as harmonics, inter-harmonics, flicker, and strongly varying reactive power demand due to these loads have been serious concerning for utilities and sensitive factories. These parameters are power quality (PQ). Hence, the EAF modeling is very important to study the power system. So far, different arc model was parented by researchers. A voltage-source model is used [1-2], where voltage is considered as square waves with modulated amplitude. A two-step optimization technique to identify the arc furnace parameters considering the stochastic nature of the arc length is analyzed [3]. This method is based on a genetic algorithm (GA) which adopts the arc current and voltage waveforms to estimate parameters of the nonlinear time-varying model of an electric arc furnace. In the paper was presented [4], a nonlinear time-varying voltage-source model has been presented. In this model, the arc voltage is defined as a nonlinear function of the arc length. The time variation of the arc length is modeled by using deterministic or stochastic laws. The deterministic law usually assumes a sinusoidal behavior for the arc length.

A frequency-domain analysis method has been proposed in [5] that represents the arc voltage and current by their harmonic components. In this model, it is assumed that the arc furnace draws the maximum power in the fundamental frequency, which is not always true [6]. The model is simple; however, it cannot represent the stochastic nature of the arc. The actual arc resistance can have sinusoidal or band-limited white noise variation around the reference value [7]. In [8], an arc model based on hidden Markov model (HMM) is presented. Single-phase HMM, the necessity of flicker function and lack of EAF parameters calculation, mismatch of the measured and simulated voltage waveform in the main bus are the reasons that authors tried to introduce a three phase model for EAF with minimum the transient bugs and errors in during the arc modeling in the present paper. Similarly, the deterministic model of electric arc furnace based on non-linear equations was presented in [9] which is applied in differential equations. Flicker analyzing and prediction are studied in [10]. In this paper, voltage flicker effects are predicted and investigated in the power system.

In this paper, regarding to disadvantage of the presented EAF model, at first step, an actual power system with EAF is designed. In this step, all EAF parameters as flexible cables, busbars, and electrodes are considered due to the accuracy in the power system modeling. Hence, power quality studies in power system in this paper are exactly related to the actual state. At the next step, a stochastic three-phase arc model in time domain is developed. The applied method is based on three-phase recovered hidden Markov model (HMM) by the use of actual measured samples in worst condition, EAF scrap melting stage. For recovering the HMM, at first, the joint transition probability is proposed. Then C factor for coupling the HMM is used and the extended parameter space in the recovered HMM is presented. The proposed model is less linear approximation matches to the measured state and shows actual flicker in which this model needs less special equations for flicker modeling. Finally, this model is compared with the measured samples in order to be assured of the operation of the presented model. Then, the effects of the operated EAF on PQ parameters of power system are studied. To study the effects of flicker, the IEC flickermeter is also designed. To implement the presented model, the actual values of EAFs of Mobarakeh Steel Company (MSC) are used and for measuring of the actual samples, the Techint digital regulators (TDR) are applied and for comparing the simulated model with actual system, the power quality analyzers are installed on the power system that is synchronous together with TDR. The simulation results show the precision and accuracy of the proposed model.

2- POWER SYSTEM WITH EAF MODELING

In order to analyze the proposed model, the power supply of arc furnace should be modeled in the actual state. Fig. 1 shows the single-line diagram (SLD) of an electric system. In this figure, bus 1 indicates the point of common coupling (PCC), T_F transformer (MV/LV) is used. This transformer has 33 tap changer located at the secondary winding to have the ability of changing the voltage of the furnace.

The transformer T_S (HV/MV) connects the EAF to PCC bus. In this figure, L_F and R_F are the inductance and resistance of the cable line connected to the furnace electrodes, respectively. The short circuit reactance at PCC bus is also shown by X_{SC} . It should be noted, EAF performance includes four stages of melting, scrap, charging DRI, plating and refining.

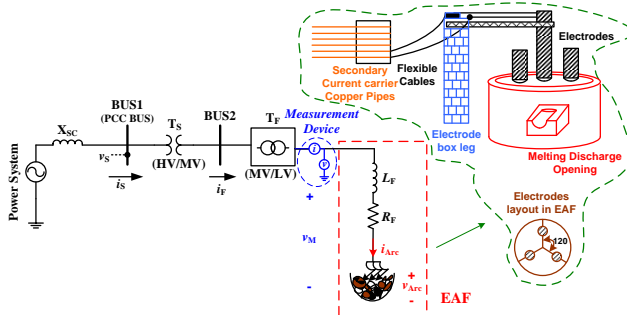


Fig. 1. Single line diagram of electric system

At the scrap, the number tap of furnace transformer (T_F) is set to middle tap. High current, short arc length and rated condition of T_F are the qualities of this stage. After 70% melted scrap, DRI charging is begun. At this stage, tap changer is set to maximum of own itself, voltage and arc length are raised and these conditions are continued until the final melting. In these stages, arc is stable and voltage and current have the minimum variation. With regard to Fig. 1, Eq. 1 is obtained:

$$v_M = L_F \frac{di_{Arc}}{dt} + R_F i_{Arc} + v_{Arc} \quad (1)$$

To measure arc voltage and current, v_M and i_{Arc} , a measurement device is used. According to the violent fluctuation of EAF, it is important to calculate different parameters of EAF's power system.

3- ELECTRIC ARC MODEL DESIGNING

A hysteresis state exists in an electric arc performance due to the current at the previous instants. After the current passage from zero, the arc current is initially low and the voltage across the arc descends i.e., the arc negative characteristic appears. After the current reaches its maximum value and at the start of its reduction, the voltage value is less than the value it had during its increase for a definite current. This case is observed in every half-period. Therefore, the electric arc consists of four major parts. According to the random characteristics of electric arc, and the arc instants dependency on that instant and previous instants, it is necessary to apply a model which can be trained by intense changes. The hidden Markov model was presented for EAF modeling in [8]. Although this model has good performance in different state, firstly, presented arc model is single phase and applied HMM should be three-phase that can show the unbalances and secondly, the HMM used has some bugs and errors which can affect on PQ parameters such as voltage flicker and harmonics. So in this paper, based on [8], a new three-phase probabilistic method for EAF modeling based on considering coupling factor for HMM is developed that has not any bugs ad errors and has faster

performance seep than the pervious model. The proposed model operates as "black box" for different EAF. In fact, the EAF model is similar to the voltage source controlled by current.

A. APPLICATION OF THREE-PHASE HIDDEN MARKOV MODEL (HMM) IN EAF MODELING

Characteristics of a three-phase HMM for the description of discontinuous data are as follows [8, 11]:

1- $(N)_{kp}$ is the number of the states present in the model: although the states in three-phase HMM are hidden. Where kp is a, b and c phases. The states are therefore named according to the elements of the set $\{1, \dots, (N)_{kp}\}$ and the system state at t time is shown by q_t .

2- $(M)_{kp}$ is the number of different observations at each state in three-phase HMM: observations suggest the modeled system output. The system outputs are considered as the set elements $(V)_{kp} = \{v_1, v_2, \dots, v_M\}_{kp}$.

3- The probability distribution of a one-stage state transfer in three-phase is shown by $(A)_{kp} = [a_{ij}]_{kp}$ so that:

$$(a_{ij})_{kp} = [P(q_{t+1} = j | q_t = i)]_{kp}, 1 \leq i, j \leq N_{kp} \quad (2)$$

In one state that there is no possibility for a transfer from state i to state j , then $(a_{ij})_{kp} = 0$.

4- There is the possibility of observations in the form of $(B)_{kp} = [b_j(k)]_{kp}$ vector where:

$$(b_j(k))_{kp} = [P(o_t = v_k | q_t = j)]_{kp}, 1 \leq k \leq (M)_{kp} \quad (3)$$

Indicating the probability of each of the observed symbols in j state $((j)_{kp} = 1, 2 \dots (N)_{kp})$.

5- The initial distribution function depicts the states in $(\pi)_{kp} = [\{\pi_i\}]_{kp}$, where:

$$\pi_i = P(q_1 = i), 1 \leq i \leq N \quad (4)$$

Therefore, in order to specify an HMM model into the number of states, there is a need for the number of observation and values of $(\pi)_{kp}, (B)_{kp}, (A)_{kp}$. A hidden Markov model is usually depicted by the compressed symbol of $(\lambda)_{kp} = [(A, B, \pi)]_{kp}$.

By having the HMM model parameters, it can be considered as a data generator (sequence of

observations) $(O)_{kp} = [(O_1, O_2, \dots, O_T)]_{kp}$. Where, O_t is one of the members of T set and V is the number of observations.

According to the unstable and random characteristic of electric arc, there are three basic problems for the application of HMM model in the design of the arc that is explained in [8]. The aim of this section is to focus on recovering HMM by coupling factor. It should be noted that the estimation problem of the past states by having the observations and the model parameters are solved by Optimization standards in which standard increases the percentage of the correctness of the separate states. Therefore, the following variable is defined to solve this problem.

$$[\gamma_t(i) = p(q_t = s_i | o, \lambda)]_{kp} \quad (5)$$

The percentage for being in state s at t time is to present o observation sequence and λ model. The above equation is simply calculable as recessive variables as follows:

$$[\gamma_t(i) = \frac{\alpha_t(i)\beta_t(i)}{p(o|\lambda)} = \frac{\alpha_t(i)\beta_t(i)}{\sum_{i=1}^N \alpha_t(i)\beta_t(i)}]_{kp} \quad (6)$$

The normal factor is written in three-phase as follows:

$$[P(O|\lambda) = \sum_{i=1}^N \alpha_t(i)\beta_t(i) = 1]_{kp} \quad (7)$$

Now, by the use of $[\gamma_t(i)]_{kp}$, it is possible to insert the separate states similar to s_t into t time [8].

The distinction problem of a method for the adjustment of $[(A, B, \pi)]_{kp}$ model parameters to maximize the observation sequence probability is an important problem. It is required to mention that there is a particular model to maximize the observation sequence probability and also there is no way for estimating the model parameters. However, $[\lambda = (A, B, \pi)]_{kp}$ can be selected in a way that $P(O|\lambda)$ is maximized. To approve the HMM parameters, it is embarked on the definition of $\zeta_t(i, j)$, probability at s_i state at t , and s_j state at $t=1$.

Therefore, the model and observations sequence are considered as the following equation:

$$[\zeta_t(i, j) = p(q_t = s_i, q_{t+1} = s_j | o, \lambda)]_{kp} \quad (8)$$

By the use of the definition of recessive variables, $[\zeta_t(i, j)]_{kp}$ can be written as follows [8]:

$$[\zeta_t(i, j) = \frac{\alpha_t(i)a_{ij}b_j(o_{t+1})\beta_{t+1}(j)}{P(O|\lambda)} = \frac{\alpha_t(i)a_{ij}b_i(O_{t=1})\beta_{t=1}(j)}{\sum_{i=1}^N \sum_{j=1}^N \alpha_t(i)a_{ij}b_j(O_{t+1})\beta_{t+1}(j)}]_{kp} \quad (9)$$

Where, the numerator is in $[P(q_t = s_i, q_{t+1} = s_j, O|\lambda)]_{kp}$ form and division calculates the desired probability value by $[P(O|\lambda)]_{kp}$. Previously, $[\gamma_t(i)]_{kp}$ was defined as the probability of being in state $[s_i]_{kp}$ at t time. Now, by the use of observation sequence and model, a relation between $[\gamma_t(i)]_{kp}$ and $[\zeta_t(i, j)]_{kp}$ can be obtained through collecting it on j . In short, the total of $[\zeta_t(i, j)]_{kp}$ on t time ($1 \leq t \leq T-1$) can be the expected transition probability matrix value from $[s_i]_{kp}$ state to $[s_j]_{kp}$ state. Therefore, it can be written as:

$$[\sum_{t=1}^{T-1} \zeta_t(i)]_{kp} = \text{The expected number from probability matrix } S_i \text{ in three-phase} \quad (10)$$

$$[\sum_{t=1}^{T-1} \zeta_t(i, j)]_{kp} = \text{The expected number from probability matrix } S_i \text{ to } S_j \text{ in three-phase} \quad (11)$$

By the use of the above relations, it is possible to create a method for the improvement of hidden Marko model parameters. The reasonable relations for π, B, A are written as follows:

$$[\pi_i = \text{Expected number of times in state } S_i \text{ at time } (t=1) = \gamma_1(i)]_{kp} \quad (12)$$

$$a_{ij} = \frac{\text{Expected number of transition from state } S_i \text{ to } S_j}{\text{Expected number of transition from state } S_i} = [\frac{\sum_{t=1}^{T-1} \zeta_t(i, j)}{\sum_{t=1}^{T-1} \gamma_t(i)}]_{kp} \quad (13)$$

$$b_j(k) = \frac{\text{Expected number of times in state } j \text{ and observing parameter}}{\text{Expected number of times in state } j} \quad \text{in three-phase} \\ = [\frac{\sum_{t=1}^T \gamma_t(j)}{\sum_{t=1}^T \gamma_t(j)}]_{kp} \quad (14)$$

An optimal solution, for instance, is $\arg \max_S P(S|O, \lambda)$ and the difficult problem, is on how to choose an 'optimal' set of parameters for the model given some observation sequences. Usually, the parameters are adjusted iteratively to maximize $P(O|\lambda)$. In this paper, first, the objective function $P(O|\lambda)$, that the learning algorithms try to optimize, is separate for each single HMM model. More complex objective functions have been proposed but can not take advantage of the fast

Expectation-Maximization (EM) algorithm. Second, the separate HMM models are not able to capture the interactions among different models. So it is tried to solve problems and reduce the bugs and errors for EAF modeling. This method introduces some parameters to directly capture the interaction and tries to reduce the number of transition parameters in a reasonable way. So, to model the joint transition probability as

$$P(S_t^{(c)} | S_{t-1}^{(1)}, S_{t-1}^{(2)}, \dots, S_{t-1}^{(C)}) = \sum_{c'=1}^C \theta_{c'c} P(S_t^{(c')} | S_{t-1}^{(c')}) \quad (15)$$

Where $\theta_{c'c}$ is the coupling weight from model c' to model c , i.e. how much $S_{t-1}^{(c')}$ affects the distribution of $S_t^{(c)}$ and how it affects is controlled by $P(S_t^{(c')} | S_{t-1}^{(c')})$. In other words, the joint dependency is modeled as a linear combination of all marginal dependencies. An interpretation for this formulation is presented as follows :

$$\begin{aligned} P(y|x_1, x_2, \dots, x_C) &= \frac{P(y, x_1, x_2, \dots, x_C)}{P(x_1, x_2, \dots, x_C)} = \\ \frac{P(x_1)P(y|x_1)P(x_2|y, x_1)\dots P(x_C|y, x_1, x_2, \dots, x_{C-1})}{P(x_1, x_2, \dots, x_C)} &= w_1 P(y|x_1) \end{aligned} \quad (16)$$

$$P(y|x_1, x_2, \dots, x_C) = w_1 P(y|x_1) = w_2 P(y|x_2) = \dots = w_C P(y|x_C) \quad (17)$$

with $\{w_c\}_{c=1,2,\dots,C}$ as appropriate factors that capture the complex dependencies between y and x 's. Finally, the joint conditional probability can be rewritten as

$$P(y|x_1, x_2, \dots, x_C) = \sum_{c=1}^C \theta_c P(y|x_c) \quad (18)$$

Where $\theta_c = \frac{1}{C} w_c$, $1 \leq c \leq C$ which are the parameters used to show the interactions among different models. Of course, the new model still contains more parameters than the previous HMM [8]. Precisely, the recovered HMM (called RHMM) has C^2 transition probability matrices (compared to C in C previous HMM) and one more coupling matrix Θ . In short, the recovered HMM is reasonable and easier than the C previous HMM. For enlarging RHMM formulation, there are assumed C s in HMM, the parameter space consists of the following components:

- prior probability $\pi = \{\pi_j^{(c)}\}$, $1 \leq c \leq C$, $1 \leq j \leq N^{(c)}$

$$\sum_{j=1}^{N^{(c)}} \pi_j^{(c)} = 1 \quad (19)$$

- transition probability $A = \{a_{ij}^{(c',c)}\}$, $1 \leq c', c \leq C$, $1 \leq i \leq N^{(c')}$, $1 \leq j \leq N^{(c)}$

$$\sum_{j=1}^{N^{(c)}} a_{ij}^{(c',c)} = 1 \quad (20)$$

- observation probability

$$B = \{b_j^{(c)}(k)\}, \quad 1 \leq c \leq C, \quad 1 \leq j \leq N^{(c)}, \quad 1 \leq k \leq M$$

$$\sum_{k=1}^M b_j^{(c)}(k) = 1 \quad (21)$$

- coupling factor $\Theta = \{\theta_{c',c}\}$, $1 \leq c', c \leq C$

$$\sum_{c'}^C \theta_{c',c} = 1 \quad (22)$$

Thus, the proposed new recovered HMM based on coupling factor can be characterized by a quadruplet $\lambda = (\pi, A, B, \Theta)$ where Θ is the interaction parameters new in its formulation. It can be seen that all these parameters are still subject to the stochastic constraints, which generate convenience for the later re-estimation method. All parameters can be estimated in a similar way.

For RHMM, similarly, it is tried to solve $P(O|\lambda)$ by defining the forward and backward variables. Each o_t is a vector $(o_t^{(1)} \ o_t^{(2)} \ \dots \ o_t^{(C)})^T$. Since the HMM and C factor are coupled together, the expanded forward and backward variables should be defined jointly across RHMM as:

$$\alpha_t(j_1, j_2, \dots, j_C) = P(o_1, o_2, \dots, o_t, S_t, j_1, S_t, j_2, \dots, S_t, j_C | \lambda) \quad (23)$$

And the expanded backward variable as

$$\beta_t(j_1, j_2, \dots, j_C) = P(o_{t+1}, \dots, o_T | S_t, j_1, S_t, j_2, \dots, S_t, j_C, \lambda) \quad (24)$$

Consequently, the inductive steps for these two variables are respectively

$$\begin{cases} \alpha_t(j_1, j_2, \dots, j_C) = \\ \left\{ \prod_c \pi_{j_c}^{(c)} b_{j_c}^{(c)} (o_1^{(c)}) \right. \\ \left. + \sum_{i_1, i_2, \dots, i_C} i_1, i_2, \dots, i_C \left(\alpha_{t-1}(i_1, i_2, \dots, i_C) \prod_c b_{j_c}^{(c)} (o_t^{(c)}) \sum_c \theta_{c,c} \cdot a_{i_c j_c}^{(c,c)} \right) \right\} t > 1 \end{cases} \quad (25)$$

and

$$\beta_t(j_1, j_2, \dots, j_C) = \begin{cases} 1 & t=T \\ \sum_{j_1, j_2, \dots, j_C} i_1, i_2, \dots, i_C \left(\beta_{t-1}(j_1, j_2, \dots, j_C) \prod_c b_{j_C}^{(c)} (o_{t+1}^c) \sum_{c'} \theta_{c'c} a_{i'_C j_C}^{(c', c)} \right) & t < T \end{cases} \quad (26)$$

The likelihood function $P(O|\lambda)$ can also be solved as

$$P(O|\lambda) = \sum_{j_1, j_2, \dots, j_C} \alpha_T(j_1, j_2, \dots, j_C) = \sum_{j_1, j_2, \dots, j_C} \alpha_T(j_1, j_2, \dots, j_C) \beta_T(j_1, j_2, \dots, j_C) \quad \forall t \quad (27)$$

Therefore, by a proper application of recovered HMM model on the basis of the expressed explanations and the use of the actual measured data of the electric arc, it is possible to have access to a new three-phase model on the basis of the actual data. In order to model this arc, the proposed arc is modeled in the form of a voltage source dependent on the input current and the voltage value of its two ends is related to the arc input current. Briefly, Fig. 5 shows the block diagram of the purposed three-phase model.

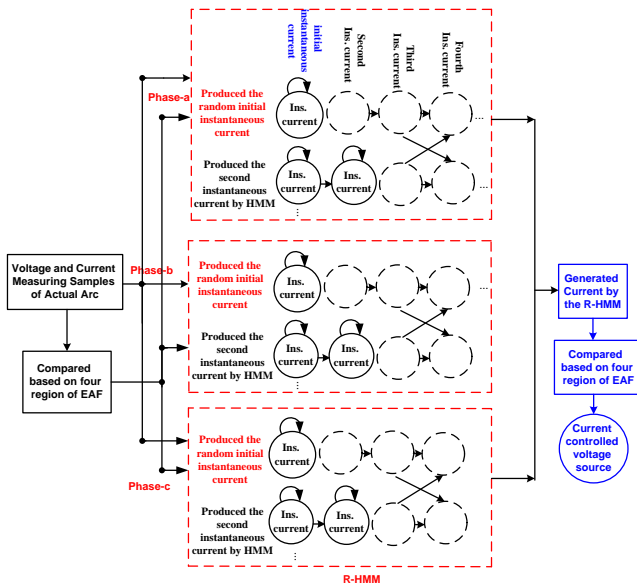


Fig. 5. Block diagram of purposed model

4- EXPERIMENTAL RESULTS

A. VALIDATIONS OF THE PROPOSED ARC MODEL

For accurate analysis of the proposed model, MSC is selected. MSC is one of the largest factories producing steel in the steel industries. In this plant, eight EAFs are used. EAF performance includes four stages of melting, scrap, charging DRI, plating and refining, the worst conditions is scrap stage. At this stage, tap number of furnace transformer (T_F) is set to 23. High current (80 kA), short arc length and rated condition of T_F are qualities of this stage. After 70% melted scrap, DRI charging is begun. At this stage, tap changer is set to the

maximum of own itself (tap=33), voltage and arc length are raised and these conditions are continued until the final melting. In 2nd and 3rd stage , arc is stable and voltage and current have the minimum variation. To measure the arc voltage and current, TDR device is used, in which the TDR digital electrode regulation system uses state-of-the-art Motorola microprocessor technology to achieve a real-time regulation loop. With regard to Fig. 1, Table 1 shows the EAF calculated parameters of MSC.

TABLE 1. MSC SYSTEM PARAMETERS

Different Parameters	
Feeding System	$S_{sc} = 11000 \text{ MVA}$, $V = 400 \text{ kV}$, $X_{th} = 145 \Omega$, $f = 50 \text{ Hz}$
Furnace Transformer	Rated Power: 125 MVA Rated Voltage: 63/0.6-1.3kV kV \times U _K : %6
Arc Furnace Load	Volumes of the Flexible Cables $L_a = 4.0459 \mu\text{H}$ $R_a = 7.1 \mu\Omega$ Volumes of the Arms $L_a = 3.32 \mu\text{H}$ $R_a = 3.55 \mu\Omega$ Volumes of Electrodes $L_a = 2.37 \mu\text{H}$ $R_a = 29.7 \mu\Omega$ Final Volumes $L_{eq} = 4.0959 \mu\text{H} + 3.32 \mu\text{H} + 2.37 \mu\text{H}$ $= 9.7859 \mu\text{H}$, $X_{eq} = j3.074 \text{ m}\Omega$
System Transformer	Rated Power: HV: 130/180/220 MVA LV: 130/180/220 MVA TV: 65/90/110 MVA Rated Voltage: 400±9x1.67%/63/30.5 kV YN yno d11 $U_k\%:$ 13.9% (HV-LV, 220 MVA Base) 12.76% (HV-TV, 110 MVA Base) 5.01% (LV-TV, 110 MVA Base)
Measurement Unit (TDR)	Turn Ratio of Current Furnace Transformer (CT) 900000/5 Turn Ratio of potential Transformer (PT) 63000/1000 Sampling rate 2000 Hz

MSC is one of the largest factories producing steel in the steel industries. In this plant, eight EAFs are used. EAF performance includes four stages of melting, scrap, charging DRI, plating and refining, the worst conditions is scrap stage.

Fig. 6 shows the different EAF characteristics on T_F secondary basis on the use of RHMM model and the actual measured samples by considering the effects of EAF in Fig. 1. As it is observed, after re-reading the data by the proposed model, this model is trained in the all states (see Fig. 7) and the electric arc approaches to the actual measured data. Hence, Fig. 6(a) shows the V-I characteristics of EAF in tree-phase. After training, in order to study the conformity rate of the proposed model and the experimental result, Fig. 6(b) and 6(c) show the

arc voltage and current changes in the actual measured and the proposed model. With regard to Fig. 6(b), it is observed that the arc voltage is very close to the actual data. In the same manner, the electric arc current conforms to the measured state according to fig. 6(c). For more accurate investigating of proposed model and actual data, Fig. 6(d) and 6(e) show the voltage and current in the experimental and estimating model in phase-a.

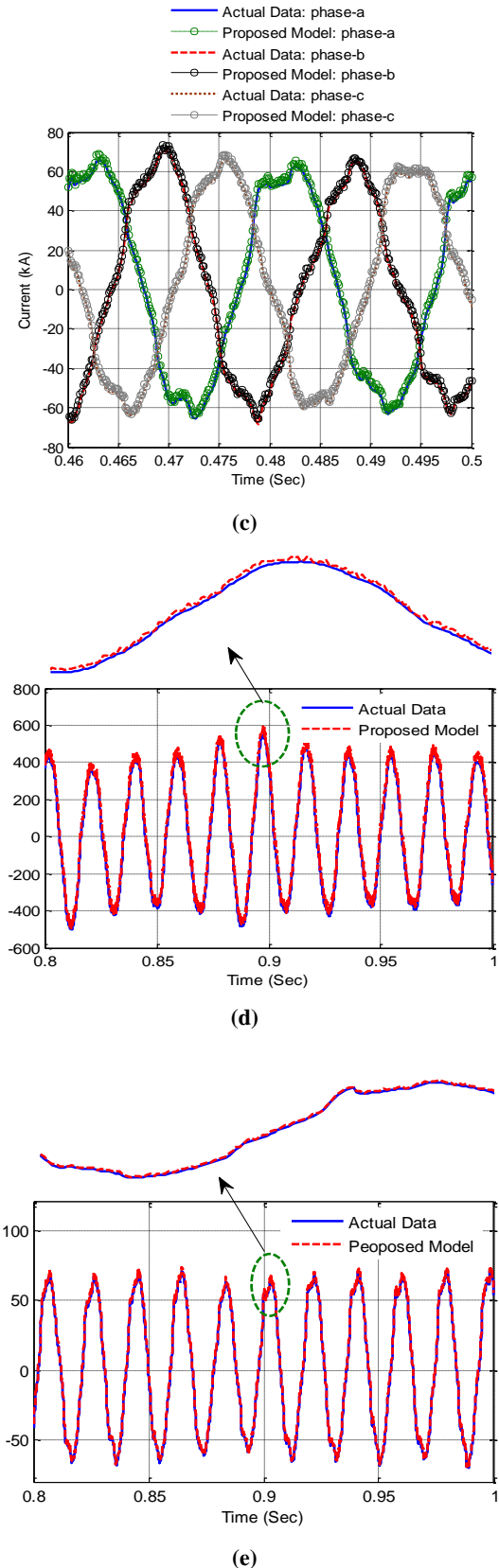
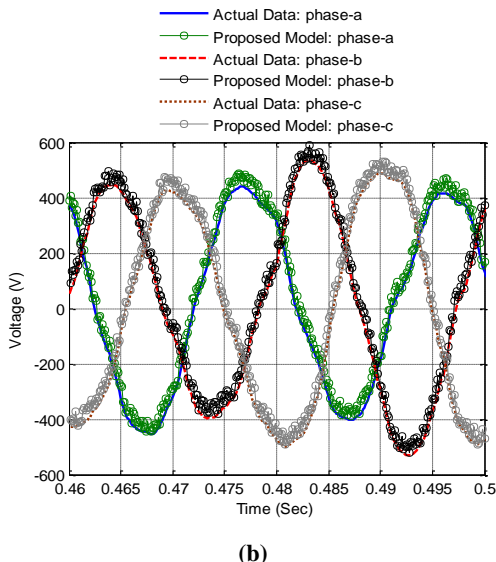
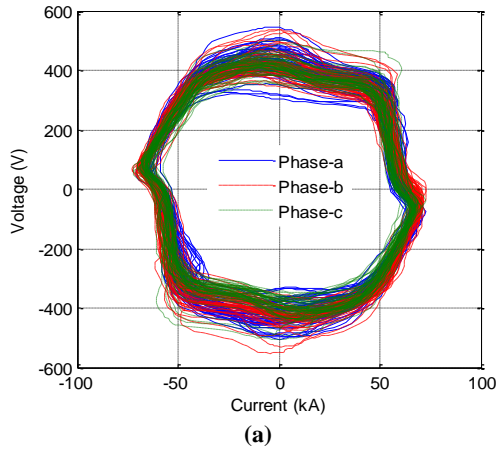


Fig. 6. Electric arc voltage and current changes in actual and proposed model:
 a) V-I characteristic. b) Three- phase voltage curve. c) Three- phase current curve. d) voltage changes in phase-a. e) current changes in phase-a.

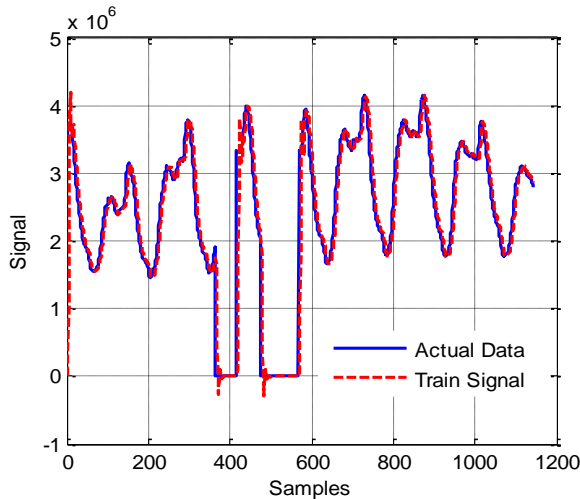


Fig. 7. Training proposed model based on actual data

Similarly, according to Eq. (1), by extracting v_{arc} and i_{arc} from this equation regarding to Table 1., three phase electric arc voltage is shown in Fig. 8. As observed in figure, the proposed model is more accurate without any linearization than the other models presented in [9]. Likewise, with accurate comparing between the proposed model and model was presented in [9], it can be easily seen that the presented model is executed with any bugs and error which can affect on PQ parameters.

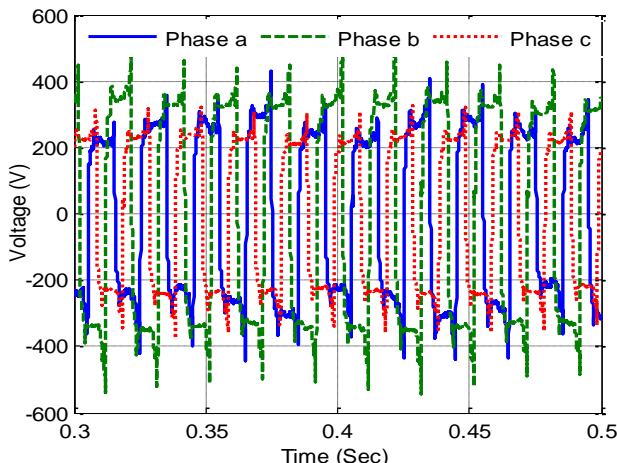
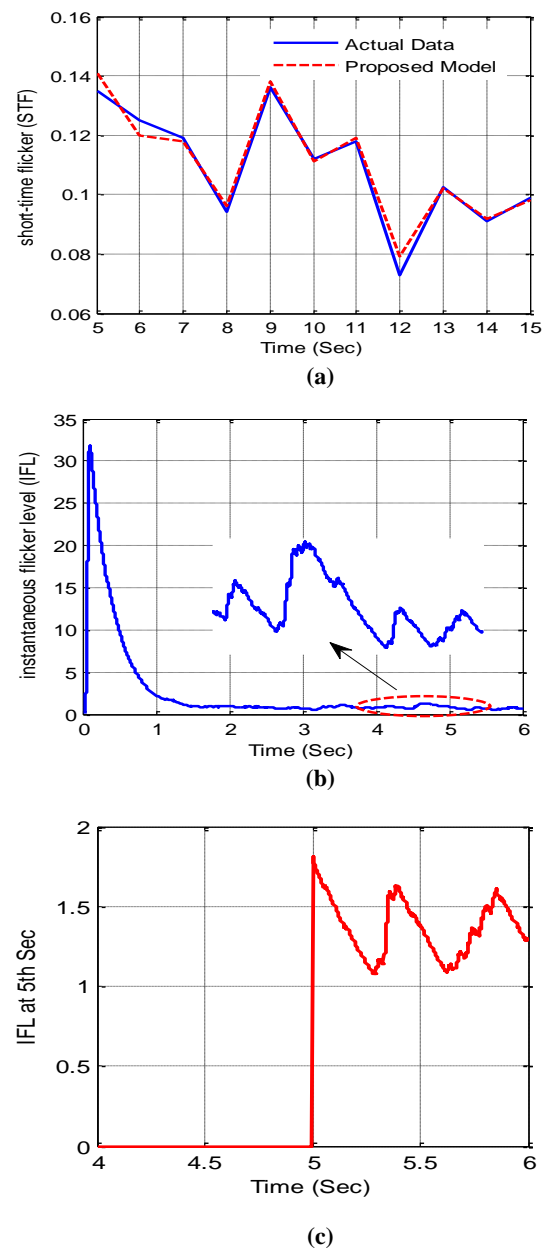


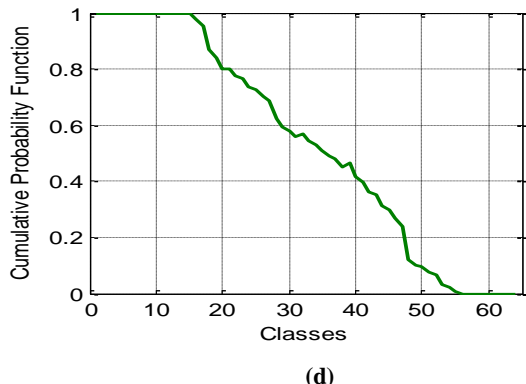
Fig. 8. Three-phase electric arc voltage

B. VERIFICATION OF PROPOSED ELECTRIC ARC MODEL IN POWER SYSTEM

For verifying the proposed arc model in the power system, two power quality analyzers (PQA), type of HIOKI3196, and 1 for data collecting are connected to PCC bus and Bus 2. Two oscilloscopes are also joined to PCC bus and EAF secondary transformer. It should be noted, these devices are synchronous together and TDR. Then, the results of the proposed model simulated in PSCAD/EMTD and MATLAB interface are compared with the experimental results. Hence, different power quality parameters such as voltage and current harmonics, voltage flicker, power factor and profile voltage are compared

together. Fig. 9(a) describes the comparison of short-time flicker (STF) in measured and simulated states which is calculated by IEC flickermeter [12-13]. In this flickermeter, at first, the instantaneous flicker level (IFL) is calculated which indicates the instantaneous value of flicker at any moment. Then, cumulative probability function (CPF) is recognized. It is required to mention that the shapes of the CPF curves are not similar to each other for all the different types of flicker generating loads, and have great dependency on the type of voltage fluctuations. As a result, a standard that can differentiate among these shapes and can quantitatively evaluate the flicker severity should be used. This appropriate standard is obtained through introducing the flicker short-time index and using multi-point method. Fig. 9(a), 9(b) and 9(c) show the general IFL and IFL samples and CPF at 5th second, respectively.





(d)

Fig. 9. a) Short-time flicker at PCC Bus. b) General sampled IFL. c) Sampled IFL at 5th secondary. d) The cumulative probability function (CPF) changes in terms of classification

The proposed model has been properly able to generate the flicker in bus 1 of the power system. On the one hand, the designed flickermeter has properly measured the generated flicker. To study the effects of the voltage fluctuations, fig. 10 shows the curve for the changes of voltage a-phase profile on bus 1 in the measured and simulated models.

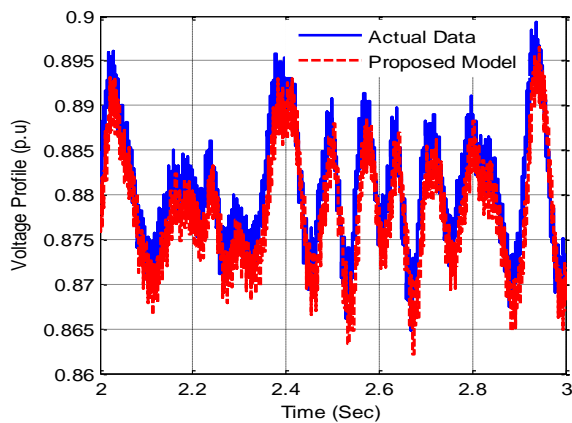


Fig. 10. The curve for changes of voltage three-phase profile in bus 1

Fig. 11 exhibits the PCC bus power factor which changes around 0.6 in the measured and simulated model. This value is changed according to voltage changes and has satisfactory conformity with actual data. Also, the frequency changes in this bus compared between experimental results and proposed model are indicated in Fig. 12.

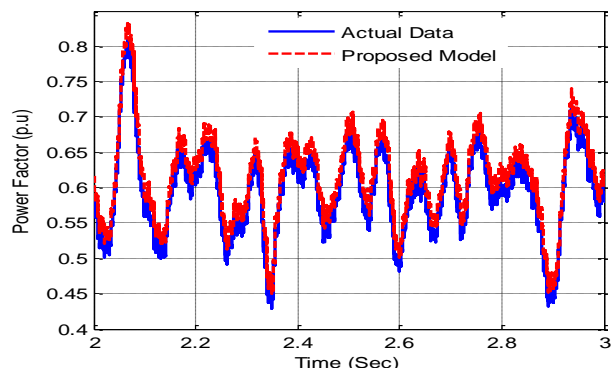


Fig. 11. Power factor changes in bus 1

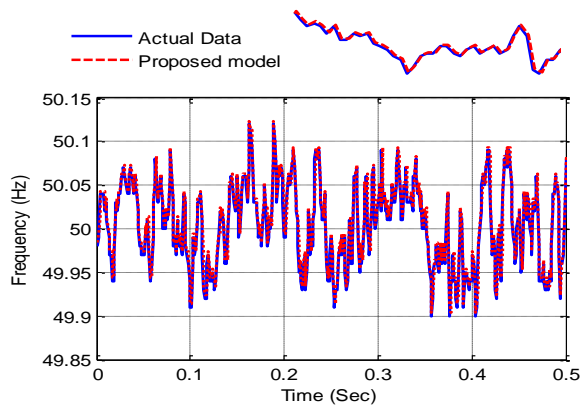


Fig. 12. Frequency changes in PCC bus

In order to study the voltage and current harmonics which have been generated by the EAF, Table 2 shows the magnitude of voltage and current harmonics, total harmonic distortion (THD) of voltage and current at bus 1. As previously mentioned, these harmonics are measured by PQA, HIOKI3196. By comparing the measured and simulation values, it is observed that the generated harmonics magnitude in the measured state has proper conformity with the proposed model.

5- CONCLUSION

In this paper, a probabilistic model for electric arc based on RHMM and actual samples of voltage and current measurements was presented. The proposed method has not any bugs and errors by applying the coupling factor in HMM. This model can be used for the power quality studying of power system with EAFs and investigating types of power system compensators as SVC, STATCOM, etc. This model can be generated in all melting stages such as scarp, DRI charging, plating and refining and operated as a black box. The presented model was probed under the most unfavorable conditions. The comparison between simulation and experimental results described the advantages of the proposed method in EAF modeling.

TABLE 2. HARMONIC ORDERS AT THREE PHASES IN THE PCC BUS

Order Harmonic	Phase a (% of Fundamental)				Phase b (% of Fundamental)				Phase c (% of Fundamental)			
	Exp.	Pro.	Exp.	Pro.	Exp.	Pro.	Exp.	Pro.	Exp.	Pro.	Exp.	Pro.
	V _a	I _a	V _b	I _b	V _c	I _c						
2	1.29	1.295	3.45	3.44	1.26	1.27	3.44	3.43	1.29	1.26	3.43	3.47
3	5.18	5.19	8.08	8.07	5.19	5.18	8.13	8.11	5.14	5.11	8.12	8.17
4	1.9	1.85	4.41	4.42	1.79	1.72	4.49	4.46	1.70	1.64	4.31	4.32
5	7.16	7.16	42.5	42.5	7.11	7.12	42.4	42.6	7.15	7.11	42.4	42.4
6	1.85	1.84	1.37	1.36	1.83	1.82	1.35	1.33	1.85	1.84	1.33	1.36
7	4.90	4.88	6.32	6.35	4.92	4.89	6.34	6.36	4.80	4.84	6.35	6.35
9	3.75	3.76	1.32	1.34	3.74	3.75	1.31	1.32	3.76	3.77	1.38	1.34
11	4.00	3.98	0.80	0.82	4.05	3.98	0.84	0.86	4.01	3.99	0.88	0.81
13	3.59	3.61	0.27	0.25	3.51	3.56	0.21	0.23	3.55	3.59	0.26	0.24
THDV	6.68	6.70			6.69	6.71			6.68	6.67		
THDI			30.5	30.45			30.4	30.35			30.6	30.56

REFERENCES

- [1] M. Alonso, M. Donsion, "An Improved Time Domain Arc Furnace Model for Harmonic Analysis", IEEE Trans. Power Del., vol. 19, No. 1, pp.367- 373, 2004.
- [2] S. G. Deaconu, N. Popa, A. I. Toma, M. Topor, "Modeling and Experimental Analysis for Modernization of 100-t EAF", IEEE Trans. on Ind. App. vol. 46, No. 6, pp.2259- 2266, 2010.
- [3] S. M. Mousavi Agah, S. H. Hosseiniyan, H. Askarian Abyaneh, N. Moaddabi, "Parameter Identification of Arc Furnace Based on Stochastic Nature of Arc Length Using Two-Step Optimization Technique", IEEE Trans. on Power Del., vol. 25, No. 4, pp. 2859- 2867, 2010.
- [4] I. Vervenne, K. Van Reusel, R. Belmans, "Electric Arc Furnace Modeling from a "Power Quality" Point of View", Electrical Power Quality Utilization IEEE Int. Conf., pp. 1-6, 2007.
- [5] W. Ting, S. Wannan, Z. Yao, "A New Frequency Domain Method for the Harmonic Analysis of Power Systems with Arc Furnace", Advances in Power System Control, Operation and Management IEEE Int. Conf., pp. 552- 555, 1997.
- [6] L. F. Beites, J. G. Mayordomo, A. Hernandes, R. Asensi, "Harmonics, Interharmonic, Unbalances of Arc Furnaces: a New Frequency Domain approach", IEEE Trans. Power Del., vol. 16, No. 4 pp. 661- 668, 2001.
- [7] L. F. Pak, V. Dinavahi, G. Chang, M. Steurer, P. F. Ribeiro, "Real-Time Digital Time- Varying Harmonic Modeling and Simulation Techniques", IEEE Trans. Power Del., vol. 22, No. 2 pp. 1218- 1227, 2007.
- [8] M. Torabian Esfahani, B. Vahidi, "A New Stochastic Model of Electric Arc Furnace Based on Hidden Markov Model: A Study of Its Effects on Power System", IEEE Trans. Power Del., vol. 27, No. 4 pp. 1893- 1901, 2012.
- [9] D. Grabowski, J. Walczak, "Deterministic model of electric arc furnace – a closed form solution", COMPEL: The International Journal for Computation and Mathematics in Electrical and Electronic Engineering vol. 32 No. 4, pp. 1428- 1436, 2013.
- [10] Y. Hsu, K. H. Chen, P. Huang, Ch. Lu, "Electric Arc Furnace Voltage Flicker Analysis and Prediction" IEEE Trans. on Ins. and Meas., vol. 60, No. 10, pp.3360- 3369, 2011.
- [11] A. M. Gonzalez, A. M. S. Roque, J. Garcia-Gonzalez, "Modeling and Forecasting Electricity Prices with Input/Output Hidden Markov Models", IEEE Trans. Power System, vol. 20, No. 1 pp. 13- 24, 2005.
- [12] E. Altintas, O. Salor, I. Cadirci, M. Ermis, "A New Flicker Contribution Tracing Method Based on Individual Reactive Current Components of Multiple EAFs at PCC", IEEE Trans. Ind. Appl., vol. 46, No. 5, pp.1746- 1754, 2010.
- [13] Testing and Measurement Techniques– Flickermeter, Functional and Design Specifications, IEC Standard, IEC 61000-4-15.